

## ELM Simulations with M3D

H.R. Strauss<sup>1</sup>, L. Sugiyama<sup>2</sup>, C.S. Chang<sup>1</sup>, G. Park<sup>1</sup>, S. Ku<sup>1</sup>, W. Park<sup>3</sup>, J. Breslau<sup>3</sup>,  
S. Jardin<sup>3</sup>

<sup>1</sup>New York University, New York, New York, USA

<sup>2</sup>MIT, Cambridge, MA, USA

<sup>3</sup>Princeton University Plasma Physics Laboratory, Princeton, New Jersey, USA  
strauss@cims.nyu.edu

Edge localized modes (ELMs) are important because they can control the loss of energy and particles at the edge of high temperature tokamak plasmas. We have carried out extended MHD nonlinear simulations of ELM crashes and subsequent relaxation of the pressure pedestal at the plasma edge using DIII-D and ITER geometry and initial profiles. Gyroviscous stabilization was found to have a relatively small effect on ELMs, which are dominated by long wavelength modes. The simulations typically show large density perturbations relative to temperature perturbations. We are also performing simulations using a kinetic model to initialize bootstrap current, pressure pedestal, and other profile data.

It is of great importance to simulate a complete ELM cycle, to understand the mechanisms and magnitude of the heat and particle loss. As an initial step, we have carried out simulations of ELM crashes using the extended MHD code M3D [1]. The simulations shown in Fig. 1 use an initial equilibrium constructed from DIII-D experimental data. The equilibrium is unstable to ideal MHD ballooning and peeling modes, driven by the edge pedestal pressure gradient and bootstrap current. The modes grow exponentially and then saturate, causing the pressure pedestal to relax. Excess pressure is carried out across the magnetic separatrix. Fig. 1 shows pressure contours in the edge region. Only the upper, outboard quadrant of the outer flux surfaces is shown for clarity. The simulation region consists of the outer part of the plasma, including the entire edge gradient region and part of the core, as well as the vacuum or open field line region,

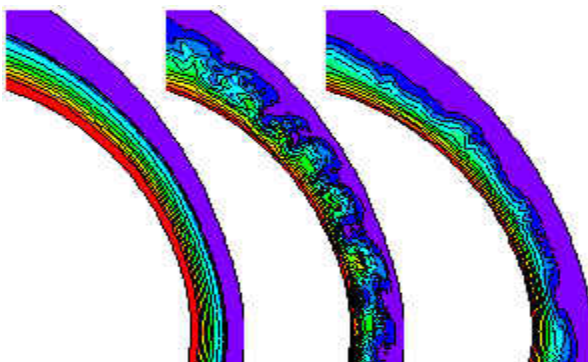


**Figure 1.** pressure at (left to right) times  $t=27t_A$ ,  
 $t=67t_A$ , and  $t=106t_A$  in a DIII-D ELM simulation.

enclosed by a conducting wall. The first part of the figure shows the equilibrium pressure at  $t=27t_A$ , where  $t_A$  is the toroidal Alfvén transit time. The core region is divided from the scrape off region by the pressure pedestal at the magnetic separatrix. The middle part of the figure shows pressure contours at  $t=67t_A$  when the unstable modes reach saturation. The mode structure is ballooning in character, having maximum amplitude on the outboard edge of plasma. The modes cause the  $n=0$  pressure gradient to relax to a stable

state, causing the modes to coalesce and decay, as shown at  $t = 106 t_A$  in the rightmost frame of Fig. 1. The open flux surface region surrounding the plasma is modeled as a highly resistive region, using a self consistent resistivity varying as temperature to the  $-3/2$  power. In these simulations the Lundquist number  $S = 10^6$  in the core, and  $S = 10^2$  outside the separatrix. This example has toroidal modes  $n = 0, 5, 10, 15, 20$ . Simulations including a more complete spectrum are qualitatively similar. Recent simulations have been carried out with all toroidal modes present up to  $n = 40$ .

The simulations presented above assumed a constant plasma density, rather than a density pedestal at the separatrix. The nonlinear advection of a steep density gradient requires special numerical methods to prevent the occurrence of negative density. We have introduced an upwinding method to deal with nonlinear numerical density evolution. The upwinding introduces a stabilizing velocity dependent effective diffusion, while still conserving flux. In the simulations we have also made a more realistic approximation of the outer boundary shape. The outer boundary condition is taken to be an ideally conducting impermeable rigid wall. We have also taken an artificial inner boundary. This boundary is a magnetic flux surface, where we assume all equilibrium quantities are fixed, and all perturbations vanish. The mesh is aligned with the equilibrium magnetic surfaces up to the separatrix. Outside the separatrix, either the mesh is aligned with an interpolation between the separatrix contour and the outer boundary, or it is completely unstructured. The initial equilibrium is perturbed with a single toroidal harmonic with mode number  $n$ . A linear eigenmode is found by an initial value simulation, which grows exponentially in time. The initial equilibrium, along with the unstable mode, is used to initialize a nonlinear simulation.

We have begun to perform simulations in ITER geometry. Some ITER simulations show a substantial outflow to the divertor. The following case shows an ITER EFIT equilibrium with a pressure pedestal, the height of which was increased to give an instability. In Fig. 2 the nonlinear pressure contours are shown near the peak amplitude of the nonlinear development at  $t = 56 t_A$ . Note the outflow to the divertor at  $t = 67 t_A$ . In the figure only the lower outboard quadrant is shown for clarity.

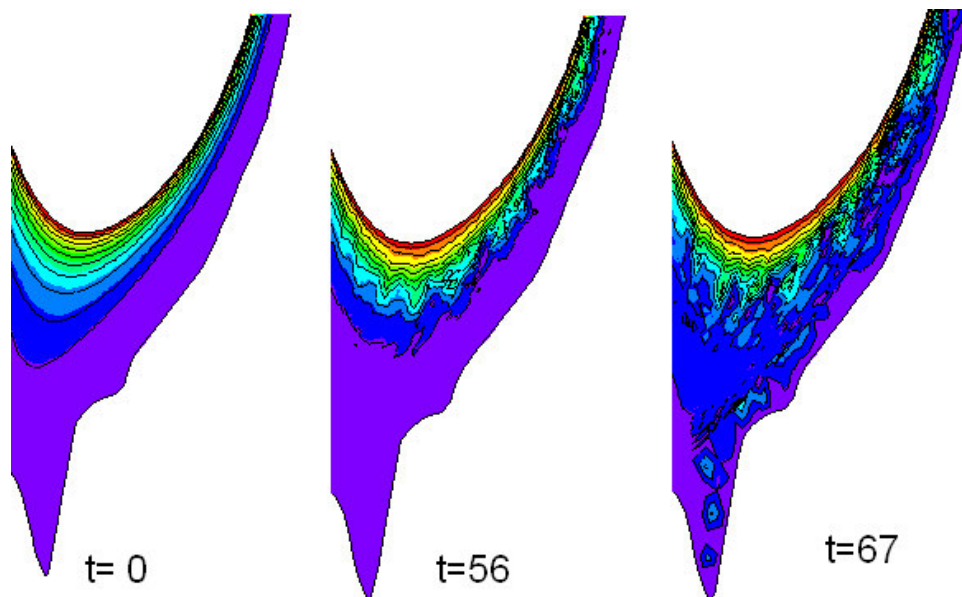


Figure 2. ELM simulation in ITER geometry. Note outflow to divertor at  $t = 67 t_A$ .

### Two Fluid Effects.

Two fluid effects simulations with M3D were focused on the stabilizing effect of gyroviscosity. The size of the two fluid effects can be measured by the Hall parameter  $H$ , the ratio of the ion skin depth to the major radius. Two fluid stabilization provides a cutoff scale below which MHD modes are stable. The gyroviscous stabilization of MHD instabilities scales as  $nH$ , where  $n$  is the toroidal mode number. We have verified this stabilization in linear simulations of  $n = 10$  ballooning modes in the edge of a DIII-D equilibrium. Fig. 3. shows the instability growth rate as the Hall parameter  $H$  is varied from 0 to 0.1. We see that the

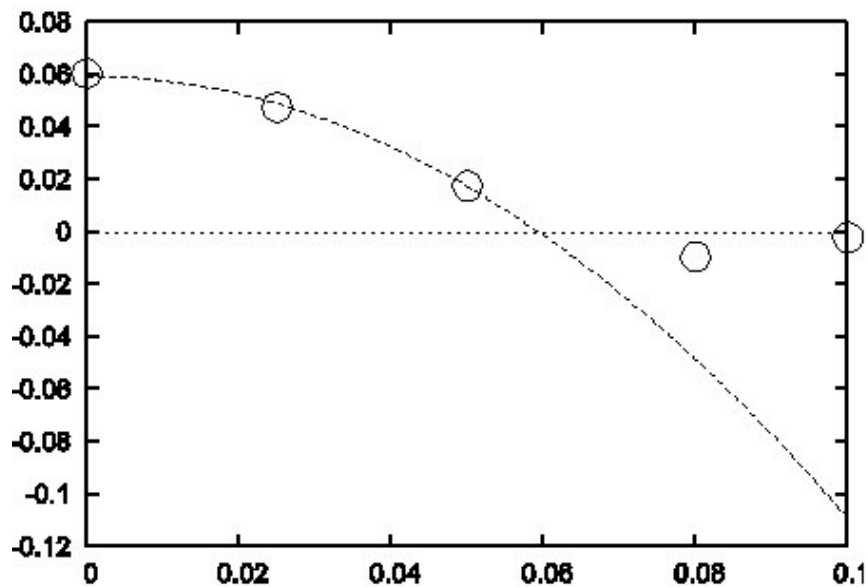
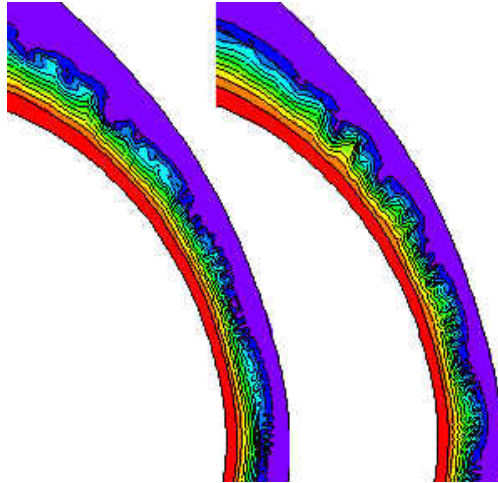


Figure 3. Growth rate of  $n = 10$  modes as the Hall parameter  $H$  is varied. The modes are stable for  $H > .06$ .

growth rate decreases with  $H$  and is zero for a critical value  $H = 0.06$ . In the nonlinear simulation of Fig. 1, the evolution is dominated by the longer wavelength modes, which are insensitive to  $H$ . Nonlinear simulations with  $H=0.03$ , which is somewhat above the experimental value (for the core density), are similar to the results of Fig.1, which were obtained with  $H = 0$ . In fact there is little difference in simulations done with MHD and two fluid models. This is shown in Fig. 4. The reason is that nonlinear simulations are dominated by moderate toroidal mode number  $n$  modes, with  $n$  around 10. These mode numbers are not affected by two fluid effects, as indicated in the linear simulations above. The two fluid effect only serve to truncate the spectrum. In the nonlinear MHD simulations, this truncation is done numerically, by limiting the number of toroidal modes included.



**Figure 4. pressure contours at  $t = 90$ . At left is MHD, at right, two fluid.**

### **Steady state profiles from kinetic calculations.**

In the above cases, the initial ideal MHD equilibrium was taken from an equilibrium reconstruction of experimental data. In other work, we use pressure profiles calculated by the neoclassical version of the XGC kinetic code [2], which is able to predict edge plasma density and pressure pedestal buildup in the plasma edge, as well as the bootstrap current. The transport based bootstrap current models used to reconstruct the initial equilibria used in the previous cases may not be good approximations at the plasma edge. Instead, kinetic profiles of the bootstrap current and pressure pedestal calculated by XGC are used to initialize a Grad Shafranov solver newly added within M3D.

The new equilibria are written out in EQDSK format. They can then be checked for MHD stability. Unstable equilibria can be evolved nonlinearly to simulate an ELM crash and pedestal relaxation, similar to the example of Fig. 1.

The following is an example computation. The initial state is a DIII-D equilibrium reconstruction, g013333, which neglects bootstrap current, and pressure and density pedestals. This initial magnetic field configuration is used by XGC to calculate bootstrap current and pressure and density pedestals. The initial EQDSK file, with magnetic field information, along with the new profiles computed by XGC, are read in by M3D. The original profiles are merged with the profiles calculated by XGC. The Grad Shafranov solver uses the profiles of the parallel current density and pressure as a function of normalized poloidal magnetic flux within the separatrix to compute a self consistent poloidal magnetic flux function. Some adjustment of magnetic flux boundary values is made in order to keep the magnetic x point from moving out of the computational

domain. An iterative solution procedure is carried out to obtain a new equilibrium with the new profiles.

The new equilibrium was then checked for linear stability. In this case modes with toroidal mode number  $n = 9$  were checked and found to be exponentially growing in time. The equilibrium and unstable mode were used to initialize a nonlinear simulation. The simulation contained toroidal modes  $n = 0, 3, 6, \dots, 21$ . Pressure contours at times  $t = 0, 25,$  and  $37 t_A$  are shown in Fig. 5. At  $t = 25 t_A$ , the ELM is near maximum amplitude. The pressure is strongly rippled at its surface, and blob like structures have formed. At  $t = 37 t_A$  the pressure is relaxing to a new stable state. It can be seen that the pressure boundary surface is less rippled, and the blobs are smaller, although the pressure shows significant turbulent perturbations. The relaxation is more evident in Fig. 6 and 7, which show profiles of density and temperature at the same three times, along the major radius

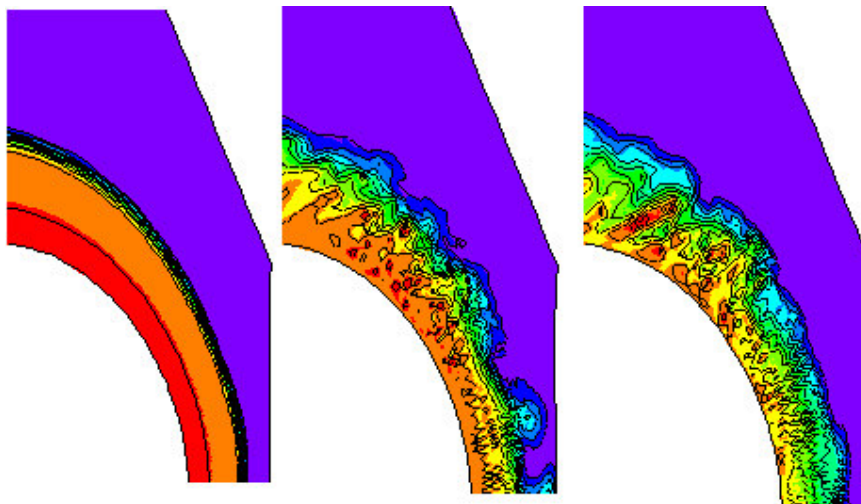


**Figure 5. Pressure contours in an ELM simulation at times  $t = 0, 25$  and  $37 t_A$  in which bootstrap current and pressure pedestal were calculated by a kinetic simulation.**

in the midplane. The profiles are not averaged. The initial state has a pedestal centered at  $R=0.5$ . It is interesting to compare the density and temperature profiles. Fig. 6 shows the density at the same times as in Fig. 5. As the density gradient relaxes, a substantial density remains outside the initial pedestal, for  $R > 0.5$ , even at  $t = 37 t_A$ . The temperature, shown in Fig. 7, is different. A large temperature perturbation occurs outside the initial pedestal at  $t = 25 t_A$ , but by  $t = 37 t_A$  the profile has already relaxed back to almost the initial  $t = 0$  temperature profile. Evidently the difference between the density and temperature is that the temperature has a large parallel thermal conduction. This equilibrates the temperature to the wall value on open field lines (the M3D model preserves pressure within flux tubes). The pressure is intermediate between density and temperature. Because the temperature quickly drops on the open field lines, the pressure is small for  $R > 0.5$  at  $t = 37 t_A$ . For  $R < 0.5$ , the pressure relaxes to a new profile, with a lesser gradient than in the initial state, which is similar to the density profile at  $t = 37 t_A$ .

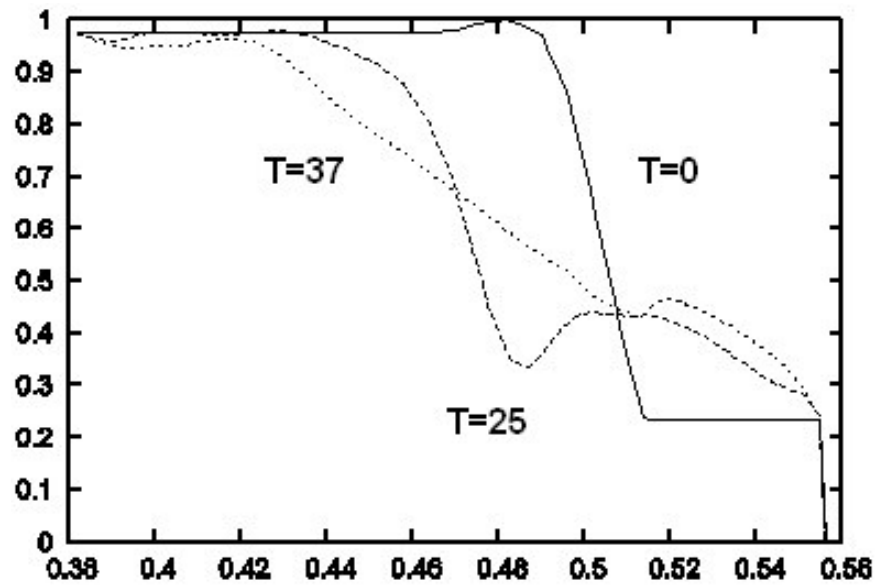


Figure 6. density profiles  $n(R)$ , at times  $t = 0, 25$ , and  $37 t_A$ .

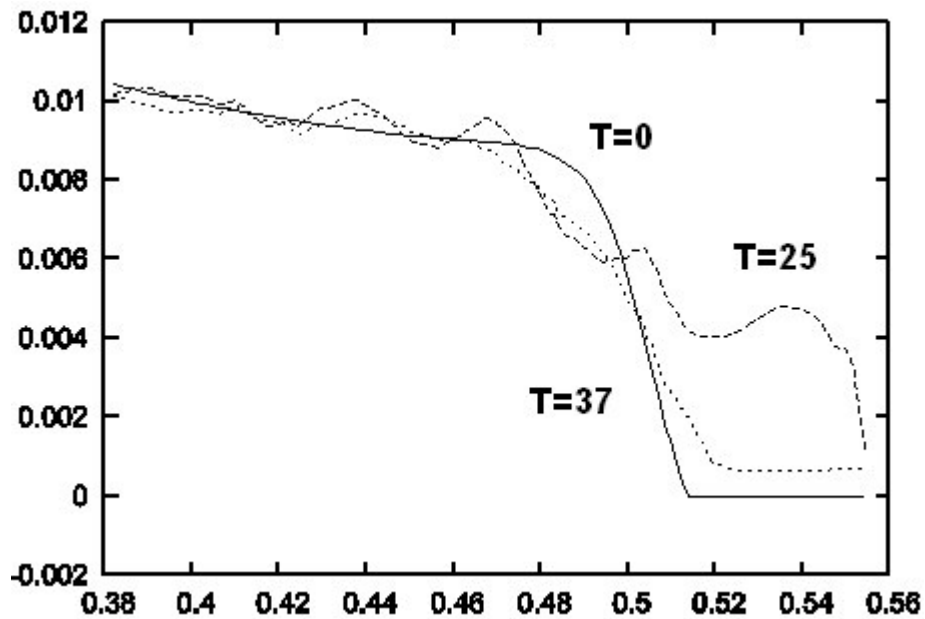


Figure 7. Temperature profile  $T(R)$  at times  $t = 0, 25, 37 t_A$ . At  $t = 25$  there is a large temperature perturbation across the separatrix, but at  $t = 37$  it has relaxed back to almost the initial  $t = 0$  temperature

## **Future Work.**

There is experimental evidence of ELM suppression [3] using applied magnetic fields. Small magnetic perturbations resonant at the  $q = 4$  magnetic surface were applied with external coils in the DIII-D experiment. It was found that this produced relatively large particle loss, but small temperature changes. There was evidence of small amplitude MHD activity. This suggests that there is MHD involvement in the ELM suppression. We plan to investigate this by combining XGC profiles with an initial EFIT equilibrium, but reducing the bootstrap current and pedestal pressure to make MHD stable equilibria. We can then examine the effects of applied external magnetic perturbations on MHD behavior.

The next stage will be to add similar magnetic perturbations to the XGC code, to see what effect the perturbations have on the pressure pedestal and bootstrap current. It is expected that this will modify the bootstrap current and pressure pedestal to make the equilibrium more stable. Then, the same resonant perturbation should have less of a response.

In other ELM computations, the time evolving magnetic field will be fed back into the kinetic computation, to self consistently calculate the changes in the profiles. Future simulations will be concerned with issues such as what distinguishes the different types of ELMs, energy and particle loss, and effects that stabilize ELMs.

This work was supported by the U.S.D.O.E.

[1] Park, W., Belova, E.V., Fu, G.Y., Tang, X.Z., Strauss, H.R., Sugiyama, L.E., Phys. Plasmas 6, 1796 (1999)

[2] Chang, C.S., Ku, S., and Weitzner, H., Phys. Plasmas 11, 2649 (2004)

[3] Evans, T. E., Burrell K. H., Fenstermacher, M. E., Moyer, R. A., Osborne, T. H., Schaffer, M. J., West, W. P., Yan, L. W., Boedo, J. A., Doyle, E. J., Jackson, G. L., Joseph I., Lasnier, C. J., Leonard, A. W., Rhodes, T. L., Thomas, P. R., Watkins, J. G., Zeng, L., The physics of edge resonant magnetic perturbations in hot tokamak plasmas, Phys. Plasmas 13, 056121 (2006).